



# HHS Public Access

Author manuscript

*Development*. Author manuscript; available in PMC 2017 August 29.

Published in final edited form as:

*Development*. 2008 October ; 135(19): 3209–3218. doi:10.1242/dev.024406.

## Mypt1-mediated spatial positioning of Bmp2-producing cells is essential for liver organogenesis

Honghui Huang<sup>1,5</sup>, Hua Ruan<sup>1,5</sup>, Meng Yuan Aw<sup>1</sup>, Alamgir Hussain<sup>1</sup>, Lin Guo<sup>1,5</sup>, Chuan Gao<sup>5</sup>, Feng Qian<sup>1</sup>, Thomas Leung<sup>2</sup>, Haiwei Song<sup>3</sup>, David Kimelman<sup>6</sup>, Zilong Wen<sup>4,\*</sup>, and Jinrong Peng<sup>1,\*</sup>

<sup>1</sup>Laboratory of Functional Genomics, 61 Biopolis Drive, Proteos, Singapore 138673

<sup>2</sup>Laboratory of Neural Differentiation and Degeneration, 61 Biopolis Drive, Proteos, Singapore 138673

<sup>3</sup>Laboratory of Translation Termination and Messenger Decay, 61 Biopolis Drive, Proteos, Singapore 138673

<sup>4</sup>Laboratory of Molecular and Developmental Immunology, Institute of Molecular and Cell Biology, 61 Biopolis Drive, Proteos, Singapore 138673

<sup>5</sup>Department of Biological Sciences, National University of Singapore, Singapore 117543

<sup>6</sup>Department of Biochemistry, University of Washington, Seattle, WA 98195-7350, USA

### Summary

Mesodermal tissues produce various inductive signals essential for morphogenesis of endodermal organs. However, little is known about how the spatial relationship between the mesodermal signal-producing cells and their target endodermal organs is established during morphogenesis. Here, we report that a mutation in the zebrafish *myosin phosphatase targeting subunit 1* (*mypt1*) gene causes abnormal bundling of actin filaments and disorganization of lateral plate mesoderm (LPM) and endoderm cells. As a result, the coordination between mesoderm and endoderm cell movements is disrupted. Consequently, the two stripes of Bmp2a-expressing cells in the LPM fail to align in a V-shaped pocket sandwiching the liver primordium. Mispositioning Bmp2a-producing cells with respect to the liver primordium leads to a reduction in hepatoblast proliferation and final abortion of hepatoblasts by apoptosis, causing the liverless phenotype. Our results demonstrate that Mypt1 mediates coordination between mesoderm and endoderm cell movements in order to carefully position the liver primordium such that it receives a Bmp signal that is essential for liver formation in zebrafish.

### Introduction

Liver organogenesis begins with the establishment of a population of hepatic precursor cells within the ventral foregut endoderm, followed by the specification of definitive hepatoblasts. The hepatoblasts delaminate from the epithelial layer to form a discrete liver bud, and

\* Authors for Correspondence: zilong@ust.hk, pengjg@imcb.a-star.edu.sg.

undergo rapid proliferation to increase the size of the bud. Finally, the hepatoblasts differentiate into functional hepatocytes and biliary duct cells (Duncan, 2003; Zaret, 2002). Based on genetic and in vitro explant studies in mouse and chick, a general picture of liver organogenesis has emerged in which the pan-endodermal transcription factors from the Foxa (Lee et al., 2005) and Gata (Zhao et al., 2005) families act in concert to establish a field of competent hepatic precursor cells (Gualdi et al., 1996), and then Fibroblast growth factors (Fgfs) from cardiogenic mesoderm (Jung et al., 1999) and Bone morphogenetic proteins (Bmps) from the septum transversum mesenchyme (Rossi et al., 2001) guide the process of hepatogenesis. In subsequent steps, Hhex acts to control the initiation and budding of the liver primordium (Bort et al., 2006), and Prox1 is crucial for the outgrowth of the liver bud and migration of hepatoblasts into the septum transversum mesenchyme (Sosa-Pineda et al., 2000). Therefore, the process of liver organogenesis is precisely controlled by a genetic network formed by liver-specific factors, pan-endodermal factors and factors from the surrounding mesodermal tissues (Duncan, 2003; Zaret, 2002).

In zebrafish, hepatoblasts are specified from an endodermal segment between the esophagus and the intestinal bulb (stomach) at 22-26 hours post-fertilization (hpf), followed by a thickening of the endodermal rod due to aggregation of the hepatoblasts at 30 hpf (Ober et al., 2003; Ober et al., 2006; Wallace and Pack, 2003). Between 26 and 30 hpf, the thickened endoderm rod along the midline shifts to the left side, accompanied by a leftward looping of the intestinal rod. This 'gut-looping' process is mediated by the asymmetric migration of the left and right lateral plate mesoderm (LPM) sheets, which generates a motive force that drives the migration of the anterior portion of the digestive system (Horne-Badovinac et al., 2003). The budding phase lasts until ~50 hpf, and is followed by a dramatic increase in liver size during the growth phase (Field et al., 2003; Ober et al., 2003; Wallace and Pack, 2003).

Pan-endodermal Gata factors (Holtzinger and Evans, 2005; Reiter et al., 1999) and the liver-specific factor Hhex (Wallace et al., 2001) play crucial roles in controlling liver organogenesis in zebrafish and other vertebrates, including mammals. Wnt2bb produced by the LPM directly adjacent to the liver-forming endoderm plays a crucial role in hepatoblast specification in zebrafish, acting to induce the expression of hhex and prox1 (Ober et al., 2006). Retinoic acid (RA), acting during gastrulation, is also necessary for the specification of hepatoblasts in zebrafish, most likely by altering the anterior-posterior identity of the mesoderm and/or endoderm (Stafford and Prince, 2002). Although these results provide an important framework for understanding liver development, it is clear that there is still much to learn about the formation of a functional liver from a field of competent endodermal cells.

Zebrafish provide an excellent system for identifying genes important for liver development (Chen et al., 2005; Mayer and Fishman, 2003; Ober et al., 2006; Sadler et al., 2005). We present here our identification and analysis of a new liverless mutant, sq181. In these mutants, hepatoblasts form initially, but the hepatoblasts fail to proliferate and they are ultimately aborted by apoptosis. The sq181 mutation is caused by an amino acid substitution in a conserved motif, KVxF, in the targeting subunit of myosin phosphatase (Mypt1), which attenuates its binding to the catalytic subunit type 1 phosphatase (PP1c; Ppp1cb - ZFIN), consequently preventing normal myosin regulation. In the sq181 mutants, morphogenesis of the LPM and liver primordium are altered, such that the LPM does not properly interact with

the liver primordium. We show that this mispositions the bmp2a-expressing LPM relative to the liver primordium, and demonstrate that the incorrect positioning of Bmp signals is the likely cause of the sq181 phenotype.

## Materials and Methods

### Fish lines

The hi2653 insertion line was kindly provided by Nancy Hopkins (Amsterdam et al., 2004). The Gut GFP line Tg(gutGFP)S584 was kindly provided by Didier Stainier (Field et al., 2003). The Tg(hsp70:dnBmpr-GFP) line is described by Pyati et al. (Pyati et al., 2005). The double line sq181;Tg(gutGFP)S584 was obtained by mating the sq181 mutant with Tg(gutGFP)S584.

### Cloning the sq181 mutant gene

The sq181 liverless mutant was isolated from a total of 524 F2 families derived from ENU (ethylnitrosourea, 3 mM)-mutagenized male fish (AB wild-type strain) by screening for liver mutants using *prox1* as the probe in a high-throughput whole-mount in situ hybridization approach. Heterozygous sq181 was mated with the polymorphic line WIK to generate the mapping population. 226 SSLP markers generated by the Fishman (Shimoda et al., 1999) and Zon (<http://zfrhmaps.tch.harvard.edu/ZonRHmapper/Maps.htm>) groups were used in bulked-segregant analysis (Shimoda et al., 1999). SSLP marker Z21636 from chromosome 4 was found to be linked to the sq181 mutation. After testing 3999 mutant embryos, the sq181 mutation was further narrowed down to between Z26623 (93 recombinants) and Z11657 (25 recombinants). These two markers were located on BAC contig 363 ([http://www.sanger.ac.uk/Projects/D\\_rerio/WebFPC/zebrafish](http://www.sanger.ac.uk/Projects/D_rerio/WebFPC/zebrafish)). Based on the BAC sequences in contig 363, new markers were designed (primer sequences for generating these SSLP and SNP markers are available upon request). Two SNP markers, SNP24 and SNP41, were found to identify 1 and 2 recombinants, respectively, within a 45 kb genomic DNA fragment containing part of the *mypt1* gene (see Fig. S1A in the supplementary material). In all work described here, the mutant genotype was determined by sequencing the PCR fragment containing the mutated base.

### Whole-mount in situ hybridization (WISH) and immunohistochemistry

For single probe WISH, probes were labeled with digoxigenin (DIG, Roche Diagnostics). Probes *prox1*, *lfabp*, *trypsin*, *insulin*, *ifabp* and *foxa1* were used as described (Chen et al., 2005; Lo et al., 2003). For *foxa2* (NM\_130949), *foxa3* (NM\_131299), *gata6* (NM\_131557) and *hhex* (NM\_130934) probes, primers were designed based on available sequence data and RT-PCR products were cloned into the pGEM-T Easy Vector (Promega). For *prox1* and *mypt1* or *prox1* and *bmp2a* double WISH, the *prox1* probe was labeled with Fluorescein (Roche Diagnostics) and the *mypt1* or *bmp2a* probe with DIG. For triple marker staining, the *hhex* RNA probe was labeled with DIG and the *insulin* RNA probe with Fluorescein. After the *hhex* and *insulin* two-color WISH, embryos were then stained with the monoclonal mouse antibody F59, which marks slow muscle (1:20 dilution, Developmental Studies Hybridoma Bank, Iowa). For sectioning, WISH embryos were embedded in OCT compound (Sakura) and cryosectioned into 14  $\mu$ m slices. A monoclonal antibody against human PKC $\zeta$

(Santa Cruz Biotechnology, CA; cat. no. sc-17781) was used as the primary antibody to detect aPKCs  $\lambda$  and  $\zeta$  in the LPM cells, followed by staining with Alexa Fluor 546-labeled secondary antibody for visualization.

### Mutant rescue

For mutant phenotype rescue, 0.5 ng of in vitro transcribed WT mypt1 mRNA (NM\_001003870) or the mutant mypt1m mRNA was injected into one-cell stage embryos. For fgf8 (NM\_131281), wnt2bb (NM\_001044344) and bmp2a (NM\_131359) rescue, full-length cDNA corresponding to these genes was obtained by RT-PCR. For mRNA injection, all mRNAs were synthesized from pCS2 plasmids using the Message Machine Kit (Ambion). For plasmid DNA injection, each target gene was cloned downstream of a functional sox17 promoter (J.P., unpublished) and then cloned into the pEGFP vector (Clontech) by replacing the GFP gene at the SacII and NotI cloning sites. One-cell stage embryos were used in injection. For RA (Sigma, USA) rescue, embryos at 9-10 hpf were incubated in egg water containing 10<sup>-8</sup>-10<sup>-7</sup> M RA (Stafford and Prince, 2002). Three days post-treatment, embryos were subjected to WISH using the DIG-labeled Ifabp probe.

### Morpholinos

Morpholinos were obtained from Gene Tools (Philomath, USA). The mypt1 morpholino (mypt1-MO, 5'-CGTAACGCAACGCTCTTCTTACCTG-3') was designed to target the junction of exon 1 and intron 1 of mypt1 and 1 nl (1.2-1.4 nmol/ $\mu$ l) was injected into one-cell stage embryos. The pp1c morpholino (PP1c-MO, 5'-AAGGAGAGAATCTAACCTACCACAG-3') was designed to target the junction of exon 2 and intron 2 of pp1c and 1 nl (0.4-0.5 nmol/ $\mu$ l) was injected.

**Mosaic analysis via cell transplantation**—Mutant donor cells were labeled by injection with 70 kDa Fluorescein-dextran (Molecular Probes) at the one-cell stage. To eliminate endodermal cells from the transplants, embryos were injected with a casanova-specific morpholino (cas-MO) (Stafford et al., 2006) together with biotin-dextran (Molecular Probes). At the 1000-cell stage, ~20 mutant donor cells or ~40 cas-MO morphant donor cells were taken and transplanted into the marginal region of a WT embryo or a mypt1-MO morphant at the same stage, respectively. Mosaic embryos were fixed at 3 dpf for WISH using DIG-labeled Ifabp RNA antisense probe. The TSA-Plus Cyanine 3/Fluorescein System (PerkinElmer) was used for detection of Fluorescein-dextran, and Alexa Fluor 488 tyramide was used with streptavidin-POD (Molecular Probes) to visualize biotin.

### RNA and protein analysis

Total RNA was extracted using TRIzol (Gibco BRL, USA). Probes were DIG-labeled and RNA gel blot hybridization was performed as described (Wen et al., 2005). For detecting the BmpR1a-GFP fusion protein, an anti-GFP antibody (1:1000, Biomed Diagnostics) was used in immunoblotting.

### Assay of the Mypt1-PP1c complex

The N-terminal 305 amino acid fragment of zebrafish and mouse Mypt1 was C-terminally FLAG-tagged and cloned into the pXJ41-FLAG vector (Yong et al., 2006). COS-7 cell transfection, co-immunoprecipitation (Co-IP) and immunoblotting were performed as described previously (Yong et al., 2006). Co-IP was performed using anti-FLAG-antibody-conjugated agarose resin (Sigma). Immunoblotting was performed using anti-HA (to detect HA-PP1c; Roche Diagnostics) and polyclonal anti-Mypt1 (Santa Cruz Biotechnology) antibodies.

### Stress fiber assay

Hela cells transfected with the FLAG-tagged zebrafish N-terminal Mypt1 1-305 were fixed and stained with an anti-FLAG primary antibody followed by Alexa Fluor 488-labeled secondary antibody. Actin fibers were stained with TRITC-labeled phalloidin (Sigma) (Yong et al., 2006).

### Heat-shock treatment

Heterozygote outcross embryos between 18 and 21 hpf were heat shocked at 40°C for 30 minutes and then transferred to 28.5°C. GFP-positive embryos were selected using a fluorescence microscope 2 hours after heat shock (Pyati et al., 2005).

### Phospho-histone H3 (P-H3) immunostaining and TUNEL assay—P-H3

immunostaining and TUNEL assay were performed as described previously (Chen et al., 2005).

## Results

### The sq181 mutation confers a liverless phenotype

We screened mutagenized zebrafish embryos using the liver-specific probe *prox1* (Ober et al., 2003) and identified the sq181 mutant. Whereas *prox1* is strongly expressed in the liver at 72 hpf in wild-type (WT) zebrafish, there was no detectable *prox1* signal at this site in sq181 mutants (Fig. 1A); the mutant also lacked expression of liver fatty acid binding protein (*lfabp*; *fabp1a* - ZFIN), a liver-specific gene (Fig. 1B). Using trypsin (exocrine pancreas) and insulin (*islet*) probes we found that although the sq181 mutant exocrine pancreas was absent (~80%) or greatly reduced in size (~20%) (Fig. 1C), the islet was unaffected (Fig. 1D). Interestingly, although partially reduced in size, the morphology of the mutant intestine was similar to that observed in the WT when examined with the intestinal marker intestine fatty acid binding protein (*ifabp*; *fabp2* - ZFIN) (Fig. 1E). Finally, the liverless phenotype was further confirmed using the pan-endodermal marker *foxa3*, which labels all the endodermal organs (Fig. 1F).

### The sq181 mutation does not block hepatic competency

The failure of liver development in the sq181 mutant could be due to an inability of endodermal cells to become competent hepatic cells. To test this, we examined the expression of *foxa1*, *foxa2*, *foxa3* and *gata6*, four factors required for the establishment of

competent hepatic cells (Lee et al., 2005; Zhao et al., 2005). At 24 hpf, no difference between the WT and mutant was discernible (data not shown), demonstrating that the initial expression of these competency genes was not affected by the sq181 mutation. Previous reports have shown that at 30 hpf, endoderm cells under the first somite thicken to form a bulge from which the liver develops (Ng et al., 2005; Ober et al., 2003; Wallace and Pack, 2003). We refer to this bulge as the liver primordium. At 30 hpf, the expression patterns of *foxa1*, *foxa2*, *foxa3* and *gata6*, including their expression in the liver primordium, were very similar in mutant and WT embryos, except that the liver primordium appeared to be positioned slightly more posterior in the mutant at this stage (Fig. 2). At 34 hpf, both the WT and sq181 mutant continued to express *foxa1*, *foxa2*, *foxa3* and *gata6* in the liver primordium. However, whereas the WT liver primordium forms a discrete bud at 34 hpf, the shape and size of the liver primordium in the mutant at 34 hpf was almost the same as that observed at 30 hpf (Fig. 2). In addition, the mutant liver primordium appeared to be positioned more posteriorly than that in the WT (Fig. 2). At 48 hpf, the mutant had little or no detectable expression of *foxa1*, *foxa3* and *gata6* in the liver primordium, but expression was clearly detectable in other parts of the digestive organs, except for the pancreatic bud (Fig. 2; *foxa2* expression was undetectable in the liver at 48 hpf in WT and mutant). Therefore, the sq181 mutant does initiate the expression of the genes required for the endodermal cells to become competent hepatic cells at around 30 hpf.

### **The sq181 mutant hepatoblasts are impaired in proliferation and subsequently undergo apoptosis to cause the liverless phenotype**

We next asked whether failure of liver development in the sq181 mutant is due to a failure in the specification of hepatoblasts from competent hepatic endoderm cells. *prox1* and *hhex* are the earliest markers for definitive hepatoblasts (Ober et al., 2006). We examined the expression of these genes and found that both *prox1* and *hhex* displayed similar expression patterns in the liver primordia of WT and sq181 embryos at 30 hpf (Fig. 2). After this time, however, their expression in WT and mutant embryos diverged. Whereas the *hhex*- and *prox1*-positive cells in WT embryos continued to increase in number at 34 and 48 hpf, forming a discrete bud on the left side of the embryo, in sq181 mutants the expression of these genes never increased beyond that observed at 30 hpf, or even decreased (Fig. 2). Thus, although sq181 mutants initially induce the hepatoblast fate, they are unable to sustain it.

We then examined the terminal fate of these hepatoblasts. We first performed immunostaining using an antibody against phospho-histone H3 (P-H3), a marker of proliferating cells. Examining sectioned embryos at 30 hpf we found that the mutant had ~3-fold fewer P-H3-positive cells than did WT in the liver primordium region (10.6 cells in WT versus 3.5 cells in mutant from 6 sections per embryo; n=5 WT and n=6 mutant), while in the same sections we found only a 1.4-fold decrease of P-H3-positive cells in the mutant neural tube as compared with WT (61.8 cells in WT versus 45.5 cells in the mutant from 6 sections per embryo; Fig. 3A,B). Since there was not an obvious size difference between the WT and mutant liver primordium at 30 hpf (Fig. 2), this result suggests that the proliferation of hepatoblasts beginning at 30 hpf in the mutant was severely impaired, leading to reduced liver size at later stages. Next, we examined apoptotic activity by the TUNEL assay in the

liver primordium region of WT and sq181 mutant at 38 hpf. The mutant hepatoblasts and part of the LPM cells adjacent to the liver primordium underwent active cell apoptosis (Fig. 3C,D), whereas almost no apoptotic cells were observed in the same region in WT embryos. Our results indicate that an initial reduction in cell proliferation and ultimately programmed cell death lead to the liverless phenotype in sq181.

### The sq181 mutation alters an essential motif in Mypt1

Bulked-segregant analysis (Shimoda et al., 1999) linked the sq181 mutation to the simple sequence length polymorphism (SSLP) marker z21636 on chromosome 4. Successive use of a series of markers ultimately placed the mutation between two single nucleotide polymorphism (SNP) markers, SNP24 and SNP41, which span a 45 kb interval containing the first exon and part of the first intron of the zebrafish mypt1 gene (see Fig. S1A in the supplementary material). Sequencing exon 1 of mypt1 in sq181 identified a single nucleotide (G to A) substitution (see Fig. S1B in the supplementary material) that converts Val36 (V36) to Met36 (M36) in the KV36xF motif of Mypt1 (see Fig. S1C in the supplementary material), which is involved in binding PP1c (see below). Sequencing the remainder of the mypt1 gene revealed no other mutations (data not shown).

The hi2653 zebrafish line generated by Nancy Hopkins' laboratory was found to have the mutagenic viral vector inserted in the first intron of the mypt1 gene (see Fig. S2A in the supplementary material), but this line was not previously reported to exhibit a liver defect (Amsterdam et al., 2004). We found that the hi2653 homozygotes also displayed a liverless phenotype (data not shown). Genetic complementation tests showed that sq181 and hi2653 are allelic (Fig. 4A), and therefore these two alleles are designated as mypt1sq181 and mypt1hi2653, respectively. The mutant phenotype was also phenocopied in morphants injected with a splice-blocking mypt1-specific antisense morpholino (mypt1-MO) (Fig. 4B) (297 liverless and 26 small liver out of 323 morphants examined). Finally, we injected mRNA encoding WT and mutant Mypt1 into one-cell stage sq181 mutant embryos. At 3 days post-fertilization (dpf), 93% of the mutants injected with the WT mypt1 mRNA had the expression of lfabp restored (n=45), whereas the G-to-A mutant mypt1m mRNA failed to rescue the mutant phenotype (n=15) (see Fig. S1D in the supplementary material). These results unequivocally prove that the V36 to M36 substitution in the mypt1 gene is responsible for the mypt1sq181 liverless phenotype.

### Knockdown of PP1c also causes a liverless phenotype

Myosin phosphatase is an enzyme that dephosphorylates the smooth muscle/non-muscle myosin II regulatory light chain, which thereby inhibits myosin contraction. Myosin phosphatase is composed of three subunits: a catalytic subunit of type 1 phosphatase (PP1c), a targeting subunit (Mypt1), and a small subunit of unknown function (M20) (Ito et al., 2004; Terrak et al., 2004). A defect in Mypt1 could result in the accumulation of phosphorylated myosin owing to inefficient dephosphorylation of the myosin regulatory light chain by PP1c (Lee and Treisman, 2004; Xia et al., 2005). The accumulated phosphorylated myosin would produce excessive contractile force resulting in abnormal cell movement, causing the liverless phenotype. If this were the case, then reduction of PP1c levels would be expected to mimic the mypt1 mutant phenotype. Alternatively, because less

PP1c is bound to the mutant Mypt1 there would be more unbound PP1c in the cytosol, which might cause increased dephosphorylation of targets other than myosin and, thereby, the liverless phenotype (Xia et al., 2005). If this were the case, then reduction of PP1c levels would rescue the mypt1sq181 mutant phenotype. A pp1c splice-blocking antisense morpholino (PP1c-MO) that produces a truncated PP1c was designed to reduce the levels of endogenous PP1c (see Fig. S2B in the supplementary material). Analysis of the liver using an lfabp probe showed that injection of PP1c-MO did not rescue the liver defect in the mutant embryos (data not shown). Instead, PP1c-MO morphants resembled the mypt1sq181 mutant and were either liverless (47%, n=92) or had a small liver (53%) (Fig. 4C). This observation indicates that the liverless phenotype in mypt1sq181 is due to unregulated myosin phosphorylation.

### The mutant Mypt1 binds PP1c poorly and is functionally attenuated

Structural analysis has shown that Mypt1 binds to PP1c via its N-terminus, which contains the essential KVxF motif (Ito et al., 2004; Terrak et al., 2004). Molecular modeling based on the known structure of the chicken Mypt1-PP1c complex has shown that all five possible conformations of Met in the M36-Mypt1 mutant protein are involved in steric clashes with the pocket of PP1c that binds the KVxF motif (Egloff et al., 1997; Terrak et al., 2004), which is expected to disfavor high-affinity binding of Mypt1 to PP1c (see Fig. S3A,B in the supplementary material). To test this prediction, FLAG-tagged zebrafish and mouse WT and M36-mutant Mypt11-305 proteins were co-expressed with HA-tagged mouse PP1c in COS-7 cells. Co-immunoprecipitation analysis showed that the WT Mypt11-305 exhibited strong binding to PP1c, whereas the binding of M36-Mypt1 to PP1c was significantly reduced (Fig. 4D). In adherent cultured cells, bundles of actin filaments form contractile stress fibers in response to growth factors and mechanical stress. Disassembly of these fibers can be achieved by overexpressing PP1c and Mypt1, which is a useful way to monitor the activity of the myosin phosphatase complex in vitro (Ito et al., 2004; Xia et al., 2005). We predicted that the compromised binding of PP1c to M36-Mypt1 would be likely to lead to compromised disassembly of actin stress fibers by PP1c (Xia et al., 2005). Indeed, whereas HeLa cells transfected with zebrafish WT Mypt11-305 (42 positive cells examined) lose almost all of their stress fibers (Yong et al., 2006), cells transfected with M36-Mypt11-305 (56 cells examined) maintained a similar level of stress fibers as untransfected controls (Fig. 4E). The mypt1sq181 mutation causes abnormal aggregation of actomyosin filaments in both LPM and endoderm cells

To understand how unregulated myosin phosphorylation leads to a liverless phenotype in mypt1sq181 mutants, we first determined which tissues express mypt1 during the early stages of zebrafish development. Northern blot analysis revealed that mypt1 transcripts were expressed at similar levels from unfertilized eggs (maternal expression) through to 5-dpf embryos (Fig. 5A). Whole-mount in situ hybridization (WISH) showed that at 24 hpf, mypt1 is mainly expressed in the head and somites (Fig. 5B). At 30 and 34 hpf, mypt1 transcripts are mainly enriched in the head region and are also expressed along the foregut endoderm (Wallace and Pack, 2003) (Fig. 5B). Sectioned 34-hpf embryos hybridized with a mypt1 probe (Fig. 5C), or with mypt1 and prox1 double probes (Fig. 5D), showed that mypt1 is



expressed in the neural tube, in the LPM surrounding the endoderm, and in the endoderm cells including hepatoblasts.

The *mypt1* expression pattern in the LPM and hepatoblasts suggested that the *mypt1sq181* mutation might alter the coordination between mesoderm and endoderm cell movements, especially during the stage of endoderm organogenesis between 26 and 30 hpf. This stage is marked by a process termed 'gut-looping', which involves a force generated by the asymmetric movement of the right and left LPMs (LPM displacement) that drives the leftward bending of the anterior portion of the endoderm, giving rise to the digestive organs. We examined the LPM and endoderm cells stained with phalloidin (Fig. 6A,B) and noticed that both LPM and endoderm cells in the *mypt1sq181* mutant accumulate larger actin filament bundles, contrasting with the smooth peripheral distribution of actin filaments in WT (Fig. 6C-F). In addition, the organization of the LPM and endoderm cell sheets was clearly disrupted in the *mypt1sq181* mutant as compared with WT. The LPM displacement was also abnormal in the *mypt1sq181* mutant (Fig. 6A-F). Interestingly, the polarization of LPM cells appeared normal in the *mypt1sq181* mutant when examined with an antibody against atypical protein kinase C  $\lambda$  and  $\zeta$ , an LPM cell polarity marker (Horne-Badovinac et al., 2003) (see Fig. S4A,B in the supplementary material). These results demonstrate that the lack of *Mypt1* function causes abnormal formation of actin fibers within the endoderm and LPM, and the disrupted morphogenesis of these tissues without altering cell polarity of the LPM.

We also examined the relative positions of the liver primordium with respect to the somites, as our initial results indicated that the liver primordium was positioned more posteriorly than normal in the mutant embryos from 30-34 hpf (Fig. 2). Using three markers, insulin (for islet), *hhex* (for hepatoblasts) and the F59 antibody (for somites) (Latimer et al., 2002), we found that in both the WT and *mypt1sq181* mutant, the islet was located under the fourth somite. However, whereas the WT liver primordium is consistently positioned under the first somite throughout the early stages of liver organogenesis, the mutant liver primordium was variably positioned under the first and second somites at 30 hpf, and under the second and third somites at 34 hpf, resulting in a shorter distance from the islet to the liver primordium at 34 hpf than in the WT (Fig. 6G,H). Therefore, the *mypt1sq181* mutation also causes a posterior shift of the liver primordium.

### **The *mypt1sq181* mutation causes the liverless phenotype in a non-cell-autonomous manner**

We have shown that *mypt1* is expressed in both endoderm and LPM cells (Fig. 5C,D). To study the cell autonomy of the liverless phenotype caused by the *mypt1* mutation, we performed cell transplant experiments and found that the *mypt1sq181* mutant donor cells retain the capacity to become hepatocytes when placed in WT recipients (observed in 5 out of 20 cases) (Fig. 7A-C), a rate comparable to the control using WT donor cells (9 out of 49 cases). We also transplanted WT mesoderm donor cells [achieved by eliminating the endoderm from the donors using a *casanova* (*sox32* - ZFIN) morpholino (*cas-MO*) (Stafford et al., 2006)] into the *mypt1*-MO morphants (Fig. 7D) and found that when the WT donor cells dominated the mesoderm in the recipients, 31 out of 65 such embryos developed a

discrete liver (Fig. 7E,F). Therefore, the *mypt1sq181* mutation causes the liverless phenotype in a non-cell-autonomous manner.

### **Ectopic *Bmp2a* expression rescues the *mypt1sq181* mutant phenotype**

The above results suggest that the gut-looping process might not only determine the position of digestive organs within a fish, but might also position an inductive signal of mesodermal origin so as to reach the liver primordium to induce liver bud formation. Abnormal LPM displacement in the *mypt1sq181* mutant might alter the normal perception of such a signal by the liver primordium, thus causing defective liver development. If this were the case, ectopically expressing this inductive signal might rescue the mutant phenotype. We tested *fgf8*, *wnt2bb*, *bmp2a* and RA because these four classes of signaling factors have been implicated in liver development in various systems (Jung et al., 1999; Ober et al., 2006; Rossi et al., 2001; Shin et al., 2007; Stafford and Prince, 2002). We injected expression plasmids or mRNA for each of these factors into one-cell *mypt1sq181* mutant embryos, or incubated the embryos in RA, and analyzed the embryos 3 dpf with the *lfabp* marker. Ectopic expression of *wnt2bb* (mRNA) or *fgf8* (expression plasmid), or incubation with RA, failed to rescue the liverless mutant phenotype (see Table S1 in the supplementary material). Importantly, injection of *bmp2a* mRNA rescued liver development in 45% of the homozygous *mypt1sq181* mutants (n=93), even though these embryos had a severely ventralized phenotype, as expected (Fig. 7G).

Our results suggested that alteration of *bmp2a* signaling is at least one of the causes of the liverless phenotype in the *mypt1sq181* mutant. To directly test this hypothesis, we temporally blocked Bmp signaling using a transgenic zebrafish line expressing a dominant-negative form of *Xenopus* Bmp receptor type 1a (*BmpR1a*) fused to GFP under the control of a heat-shock promoter (Pyati et al., 2005; Pyati et al., 2006). In embryos heat shocked between 18 and 21 hpf, the dominant-negative *BmpR1a*-GFP fusion protein was maximally expressed within 2 hours, and remained at this level for at least another 4 hours (see Fig. S5A in the supplementary material). We examined these embryos with the liver marker *lfabp* and the intestinal marker *ifabp*. Whereas the GFP- embryos had normal liver development, almost all of the heat-shocked GFP+ embryos were liverless (67 out of 70 embryos examined) or had a very small liver (3 out of 70) (see Fig. S5B in the supplementary material), an observation recently also reported by Shin et al. (Shin et al., 2007). In addition, embryos heat shocked at 24 hpf displayed a small liver phenotype (52 out of 52 embryos examined), and the position of the small liver with respect to the first somite was not obviously affected when examined with a *prox1* probe at 48 hpf (see Fig. S5C in the supplementary material), demonstrating that liver development will not proceed normally if Bmp signaling is disrupted even when the primordium is correctly positioned within the embryo. In contrast to the effects on the liver, the size of the intestine was not obviously affected in the GFP+ heat-shocked embryos (see Fig. S5D in the supplementary material). M36-Mypt1 disrupts the spatial coordination between the liver primordium and *Bmp2a*-producing cells

Our results suggested that the position of a population of cells expressing a Bmp ligand might be altered in *mypt1sq181* mutants. At 24 hpf, *bmp2a* was expressed as two stripes

symmetrically positioned on the left and right sides of the midline in WT embryos (Fig. 8A). By 30 hpf, the right stripe had moved across the midline so that both stripes were on the left side of the midline (Fig. 8B). Meanwhile, the two *bmp2a* stripes aligned along the dorsal-ventral axis on the left side of the embryo straddling the first three somites (Fig. 8B). Double in situ hybridization using *bmp2a* and *prox1* probes showed that the two *bmp2a* stripes formed a V-shaped pocket sandwiching the liver primordium (Fig. 8D). Sectioning of these embryos revealed that *bmp2a* was specifically expressed in the left and right LPM cells abutting the liver primordium in WT embryos (Fig. 8F,H,J). In the *mypt1sq181* mutant, *bmp2a* was also expressed in two stripes at 24 hpf as in WT embryos (data not shown). However, the right *bmp2a* stripe failed to migrate across the midline to join the left stripe, and thus the *bmp2a* pocket was not formed at 30 and 34 hpf (Fig. 8C,E). In addition, the peanut-shaped residual mutant liver primordium was positioned more ventrally and was separated from the *bmp2a*-expressing cells by an unidentified tissue that prevented the close apposition of the *bmp2a*-producing cells and the liver primordium (Fig. 8G,I,J).

## Discussion

Here we report that a single amino acid substitution, V36 to M36, in the highly conserved KV36xF sequence in Mypt1 leads to a liverless phenotype in zebrafish. In the *mypt1sq181* mutant, the endodermal genes necessary for liver competence are activated at normal levels, as are the two genes that mark the hepatoblast fate, *hhx* and *prox1*, demonstrating that the initial activation of the liver fate proceeds normally. However, after 30 hpf, when the liver bud starts to form, the expression of *hhx* and *prox1* is gradually lost in the mutant, and the hepatoblasts fail to proliferate and eventually undergo apoptosis, resulting in the liverless phenotype.

Mypt1 is a key component of the myosin phosphatase complex (Ito et al., 2004). Numerous reports have shown that, at the cellular level, Mypt1 regulates cell migration, adhesion and retraction by mediating dephosphorylation of phosphorylated myosin regulatory light chain (RLC). Loss-of-function or knockdown of Mypt1 causes excessive phosphorylation of RLC and abnormal F-actin accumulation and distribution (Egloff et al., 1997; Eto et al., 2005; Mitonaka et al., 2007; Okamoto et al., 2005; Szczepanowska et al., 2006; Xia et al., 2005). At the developmental level, loss-of-function of *Drosophila* Mypt (Mbs - FlyBase) causes disorganized cell sheet movement and cell shape changes because of excessive non-muscle myosin II activity, which in turn cause a failure of dorsal closure during embryogenesis (Lee and Treisman, 2004; Mizuno et al., 2002; Tan et al., 2003). In *C. elegans*, loss-of-function of Mypt1 (*mel-11*) causes shortened embryos because of excessive actomyosin contractility (Piekny et al., 2003; Wissmann et al., 1999). Our studies show that *mypt1* is expressed in the LPM and foregut endoderm in zebrafish. Analysis of phalloidin staining revealed that both LPM and endoderm cells in the *mypt1sq181* mutant accumulate larger actin filament bundles and exhibit an irregular organization of LPM and endoderm cells as compared with the WT control, which explains the observation that defective Mypt1 leads to aberrant morphogenesis of both the LPM and the liver primordium. Normally, the right LPM crosses the midline and moves ventral to the liver primordium, whereas the left LPM moves dorsal to the primordium, thus forming a V-shaped LPM pocket surrounding the liver primordium. In the mutant, the right LPM fails to cross the midline and thus the pocket fails to form.

These alterations in the morphogenesis of the liver primordium and LPM alter the relative position of these two tissues. The fact that the polarization of LPM cells appeared normal in the *mypt1sq181* mutant fits with the molecular function of Mypt1 as a regulator of a motor protein complex, and suggests that the *mypt1sq181* mutation causes abnormal LPM displacement not by altering the polarization of LPM cells, but by causing aberrant actin assembly. It would be interesting in the future to study the mechanism by which actin is organized by Mypt1.

Our cell transplantation experiments showed that the *myptsq181* mutation works in a non-cell-autonomous manner. These results suggest a failure of the hepatoblasts to receive a mesodermal signal crucial for the maintenance of the liver primordium in the mutant. Upon testing four candidate signals (Fgf8, Wnt2bb, RA and Bmp2a) that could be involved in liver maintenance, we found that ectopic expression of Bmp2a was able to completely rescue liver gene expression in the mutants, which is consistent with the observation that inhibiting Bmp expression in late embryos causes the liverless phenotype [also reported recently by Shin et al. (Shin et al., 2007)]. However, owing to the fact that we do not have a means to determine the temporal expression of the injected RNA or plasmid, we cannot rule out the possibility that Fgf8 and Wnt2bb might be able to rescue liver development in the *myptsq181* mutant.

Of major importance is the observation that the LPM cells in the vicinity of the liver primordium express *bmp2a*, and alterations in the relative position of the *bmp2a*-expressing LPM and the liver primordium in the *mypt1sq181* mutant prevent the close apposition of the Bmp2a-producing cells and the liver primordium by 30 hpf. Subsequently, the mutant hepatoblasts are impaired in proliferation and ultimately undergo apoptosis. Therefore, precise spatial positioning of the Bmp2a-expressing cells with respect to the liver primordium is essential for the proliferation of hepatoblasts, and when this is disrupted a lack of proliferation and eventual programmed cell death cause the liverless phenotype in the *mypt1* mutants. The results presented here allow us to expand our understanding of liver development in zebrafish. Under the influence of the Nodal factors, the right LPM begins to move across the midline, and then under the liver primordium (Horne-Badovinac et al., 2003). This movement not only provides the force for the looping of the liver and gut (Horne-Badovinac et al., 2003), but, as we show here, also brings *bmp2a*-expressing [and possibly Fgf-expressing as well (Shin et al., 2007)] cells next to the liver primordium. The crucial role of Mypt1, and, by extension, myosin contractility, is therefore to carefully position the liver primordium relative to the source of Bmp in the LPM and thereby maintain the hepatoblasts. These observations fit very well with studies in mouse and zebrafish that demonstrate the importance of Bmp signaling in liver development (Rossi et al., 2001; Shin et al., 2007).

It is interesting that a mutation in *mypt1* has such subtle effects. We believe that *mypt1sq181* is a near-null mutation: we find the same phenotype in the insertional mutant *mypt1hi2653*, and with a splice-blocking morpholino that targets *mypt1*. We note that there is a large maternal contribution of *mypt1*, which would allow the mutant embryo to undergo early morphogenesis without apparent defects. However, at later stages, the maternal WT Mypt1 is no longer sufficient to sustain normal development, owing either to protein degradation or

to reduced amounts of protein in individual cells, and misregulated contraction and relaxation of the actomyosin filaments in the *mypt1* mutant causes abnormal cell movement in the LPM and endoderm. We anticipate that other defects might be found in these embryos when they are examined with probes that reveal subtle alterations in the development of other embryonic structures. We observed a decrease in *hhex* expression in the *mypt1sq181* mutant, coincident with a failure of the liver primordium to move properly. *Hhex* homozygous mutants in mouse are impaired in normal endoderm movement and they fail to initiate ventral pancreatic specification and lose hepatic differentiation (Bort et al., 2004; Bort et al., 2006). It would be interesting to determine whether there is a direct link between the maintenance of *hhex* expression and the endoderm movement phenotype in the *mypt1sq181* embryos.

## Supplementary Material

Refer to Web version on PubMed Central for supplementary material.

## Acknowledgments

We thank Yanmei Liu, Hao Jin and Jin Xu for helping to generate the mutant screen population and identifying SSLP panels for mutation mapping, and Yiwen Liu, Weibin Zhang and Ivan Tan for technical help. This work is financially supported by the Agency for Science, Technology and Research (A\*STAR) in Singapore.

## References

- Amsterdam A, Nissen RM, Sun Z, Swindell EC, Farrington S, Hopkins N. Identification of 315 genes essential for early zebrafish development. *Proc Natl Acad Sci USA*. 2004; 101:12792–12797. [PubMed: 15256591]
- Bort R, Martinez-Barbera JP, Beddington RS, Zaret KS. Hex homeobox gene-dependent tissue positioning is required for organogenesis of the ventral pancreas. *Development*. 2004; 131:797–806. [PubMed: 14736744]
- Bort R, Signore M, Tremblay K, Martinez Barbera JP, Zaret KS. Hex homeobox gene controls the transition of the endoderm to a pseudostratified, cell emergent epithelium for liver bud development. *Dev Biol*. 2006; 290:44–56. [PubMed: 16364283]
- Chen J, Ruan H, Ng SM, Gao C, Soo HM, Wu W, Zhang Z, Wen Z, Lane DP, Peng J. Loss of function of *def* selectively up-regulates  $\Delta$ 113p53 expression to arrest expansion growth of digestive organs in zebrafish. *Genes Dev*. 2005; 19:2900–2911. [PubMed: 16322560]
- Duncan SA. Mechanisms controlling early development of the liver. *Mech Dev*. 2003; 120:19–33. [PubMed: 12490293]
- Egloff MP, Johnson DF, Moorhead G, Cohen PT, Cohen P, Barford D. Structural basis for the recognition of regulatory subunits by the catalytic subunit of protein phosphatase 1. *EMBO J*. 1997; 16:1876–1887. [PubMed: 9155014]
- Eto M, Kirkbride JA, Brautigan DL. Assembly of MYPT1 with protein phosphatase-1 in fibroblasts redirects localization and reorganizes the actin cytoskeleton. *Cell Motil Cytoskeleton*. 2005; 62:100–109. [PubMed: 16106448]
- Field HA, Ober EA, Roeser T, Stainier DY. Formation of the digestive system in zebrafish. I. Liver morphogenesis. *Dev Biol*. 2003; 253:279–290. [PubMed: 12645931]
- Gualdi R, Bossard P, Zheng M, Hamada Y, Coleman JR, Zaret KS. Hepatic specification of the gut endoderm in vitro: cell signaling and transcriptional control. *Genes Dev*. 1996; 10:1670–1682. [PubMed: 8682297]
- Holtzinger A, Evans T. *Gata4* regulates the formation of multiple organs. *Development*. 2005; 132:4005–4014. [PubMed: 16079152]

- Horne-Badovinac S, Rebagliati M, Stainier DY. A cellular framework for gut-looping morphogenesis in zebrafish. *Science*. 2003; 302:662–665. [PubMed: 14576439]
- Ito M, Nakano T, Erdodi F, Hartshorne DJ. Myosin phosphatase: structure, regulation and function. *Mol Cell Biochem*. 2004; 259:197–209. [PubMed: 15124925]
- Jung J, Zheng M, Goldfarb M, Zaret KS. Initiation of mammalian liver development from endoderm by fibroblast growth factors. *Science*. 1999; 284:1998–2003. [PubMed: 10373120]
- Latimer AJ, Dong X, Markov Y, Appel B. Delta-Notch signaling induces hypochord development in zebrafish. *Development*. 2002; 129:2555–2563. [PubMed: 12015285]
- Lee A, Treisman JE. Excessive Myosin activity in mbs mutants causes photoreceptor movement out of the *Drosophila* eye disc epithelium. *Mol Biol Cell*. 2004; 15:3285–3295. [PubMed: 15075368]
- Lee CS, Friedman JR, Fulmer JT, Kaestner KH. The initiation of liver development is dependent on Foxa transcription factors. *Nature*. 2005; 435:944–947. [PubMed: 15959514]
- Lo J, Lee S, Xu M, Liu F, Ruan H, Eun A, He Y, Ma W, Wang W, Wen Z, et al. 15000 unique zebrafish EST clusters and their future use in microarray for profiling gene expression patterns during embryogenesis. *Genome Res*. 2003; 13:455–466. [PubMed: 12618376]
- Mayer AN, Fishman MC. Nil per os encodes a conserved RNA recognition motif protein required for morphogenesis and cytodifferentiation of digestive organs in zebrafish. *Development*. 2003; 130:3917–3928. [PubMed: 12874115]
- Mitonaka T, Muramatsu Y, Sugiyama S, Mizuno T, Nishida Y. Essential roles of myosin phosphatase in the maintenance of epithelial cell integrity of *Drosophila* imaginal disc cells. *Dev Biol*. 2007; 309:78–86. [PubMed: 17662709]
- Mizuno T, Tsutsui K, Nishida Y. *Drosophila* myosin phosphatase and its role in dorsal closure. *Development*. 2002; 129:1215–1223. [PubMed: 11874917]
- Ng AN, Jong-Curtain TA, Mawdsley DJ, White SJ, Shin J, Appel B, Dong PD, Stainier DY, Heath JK. Formation of the digestive system in zebrafish: III. Intestinal epithelium morphogenesis. *Dev Biol*. 2005; 286:114–135. [PubMed: 16125164]
- Ober EA, Field HA, Stainier DY. From endoderm formation to liver and pancreas development in zebrafish. *Mech Dev*. 2003; 120:5–18. [PubMed: 12490292]
- Ober EA, Verkade H, Field HA, Stainier DY. Mesodermal Wnt2b signalling positively regulates liver specification. *Nature*. 2006; 442:688–691. [PubMed: 16799568]
- Okamoto R, Ito M, Suzuki N, Kongo M, Moriki N, Saito H, Tsumura H, Imanaka-Yoshida K, Kimura K, Mizoguchi A, et al. The targeted disruption of the MYPT1 gene results in embryonic lethality. *Transgenic Res*. 2005; 14:337–340. [PubMed: 16145842]
- Piekny AJ, Johnson JL, Cham GD, Mains PE. The *Caenorhabditis elegans* nonmuscle myosin genes *nmy-1* and *nmy-2* function as redundant components of the *let-502/Rho-binding kinase* and *mel-11/myosin phosphatase* pathway during embryonic morphogenesis. *Development*. 2003; 130:5695–5704. [PubMed: 14522875]
- Piyati UJ, Webb AE, Kimelman D. Transgenic zebrafish reveal stage-specific roles for Bmp signaling in ventral and posterior mesoderm development. *Development*. 2005; 132:2333–2343. [PubMed: 15829520]
- Piyati UJ, Cooper MS, Davidson AJ, Nechiporuk A, Kimelman D. Sustained Bmp signaling is essential for cloaca development in zebrafish. *Development*. 2006; 133:2275–2284. [PubMed: 16672335]
- Reiter JF, Alexander J, Rodaway A, Yelon D, Patient R, Holder N, Stainier DY. Gata5 is required for the development of the heart and endoderm in zebrafish. *Genes Dev*. 1999; 13:2983–2995. [PubMed: 10580005]
- Rossi JM, Dunn NR, Hogan BL, Zaret KS. Distinct mesodermal signals, including BMPs from the septum transversum mesenchyme, are required in combination for hepatogenesis from the endoderm. *Genes Dev*. 2001; 15:1998–2009. [PubMed: 11485993]
- Sadler KC, Amsterdam A, Soroka C, Boyer J, Hopkins N. A genetic screen in zebrafish identifies the mutants *vps18*, *nf2* and *foie gras* as models of liver disease. *Development*. 2005; 132:3561–3572. [PubMed: 16000385]
- Shimoda N, Knapik EW, Ziniti J, Sim C, Yamada E, Kaplan S, Jackson D, de Sauvage F, Jacob H, Fishman MC. Zebrafish genetic map with 2000 microsatellite markers. *Genomics*. 1999; 58:219–232. [PubMed: 10373319]

- Shin D, Shin CH, Tucker J, Ober EA, Rentzsch F, Poss KD, Hammerschmidt M, Mullins MC, Stainier DY. Bmp and Fgf signaling are essential for liver specification in zebrafish. *Development*. 2007; 134:2041–2050. [PubMed: 17507405]
- Sosa-Pineda B, Wigle JT, Oliver G. Hepatocyte migration during liver development requires Prox1. *Nat Genet*. 2000; 25:254–255. [PubMed: 10888866]
- Stafford D, Prince VE. Retinoic acid signaling is required for a critical early step in zebrafish pancreatic development. *Curr Biol*. 2002; 12:1215–1220. [PubMed: 12176331]
- Stafford D, White RJ, Kinkel MD, Linville A, Schilling TF, Prince VE. Retinoids signal directly to zebrafish endoderm to specify insulin-expressing beta-cells. *Development*. 2006; 133:949–956. [PubMed: 16452093]
- Szczepanowska J, Korn ED, Brzeska H. Activation of myosin in HeLa cells causes redistribution of focal adhesions and F-actin from cell center to cell periphery. *Cell Motil Cytoskeleton*. 2006; 63:356–374. [PubMed: 16607629]
- Tan C, Stronach B, Perrimon N. Roles of myosin phosphatase during *Drosophila* development. *Development*. 2003; 130:671–681. [PubMed: 12505998]
- Terrak M, Kerff F, Langsetmo K, Tao T, Dominguez R. Structural basis of protein phosphatase 1 regulation. *Nature*. 2004; 429:780–784. [PubMed: 15164081]
- Wallace KN, Pack M. Unique and conserved aspects of gut development in zebrafish. *Dev Biol*. 2003; 255:12–29. [PubMed: 12618131]
- Wallace KN, Yusuff S, Sonntag JM, Chin AJ, Pack M. Zebrafish *hhex* regulates liver development and digestive organ chirality. *Genesis*. 2001; 30:141–143. [PubMed: 11477693]
- Wen C, Zhang Z, Ma W, Xu M, Wen Z, Peng J. Genome-wide identification of female-enriched genes in zebrafish. *Dev Dyn*. 2005; 232:171–179. [PubMed: 15580633]
- Wissmann A, Ingles J, Mains PE. The *Caenorhabditis elegans* *mel-11* myosin phosphatase regulatory subunit affects tissue contraction in the somatic gonad and the embryonic epidermis and genetically interacts with the Rac signaling pathway. *Dev Biol*. 1999; 209:111–127. [PubMed: 10208747]
- Xia D, Stull JT, Kamm KE. Myosin phosphatase targeting subunit 1 affects cell migration by regulating myosin phosphorylation and actin assembly. *Exp Cell Res*. 2005; 304:506–517. [PubMed: 15748895]
- Yong J, Tan I, Lim L, Leung T. Phosphorylation of myosin phosphatase targeting subunit 3 (MYPT3) and regulation of protein phosphatase 1 by protein kinase A. *J Biol Chem*. 2006; 281:31202–31211. [PubMed: 16920702]
- Zaret KS. Regulatory phases of early liver development: paradigms of organogenesis. *Nat Rev Genet*. 2002; 3:499–512. [PubMed: 12094228]
- Zhao R, Watt AJ, Li J, Luebke-Wheeler J, Morrissey EE, Duncan SA. GATA6 is essential for embryonic development of the liver but dispensable for early heart formation. *Mol Cell Biol*. 2005; 25:2622–2631. [PubMed: 15767668]

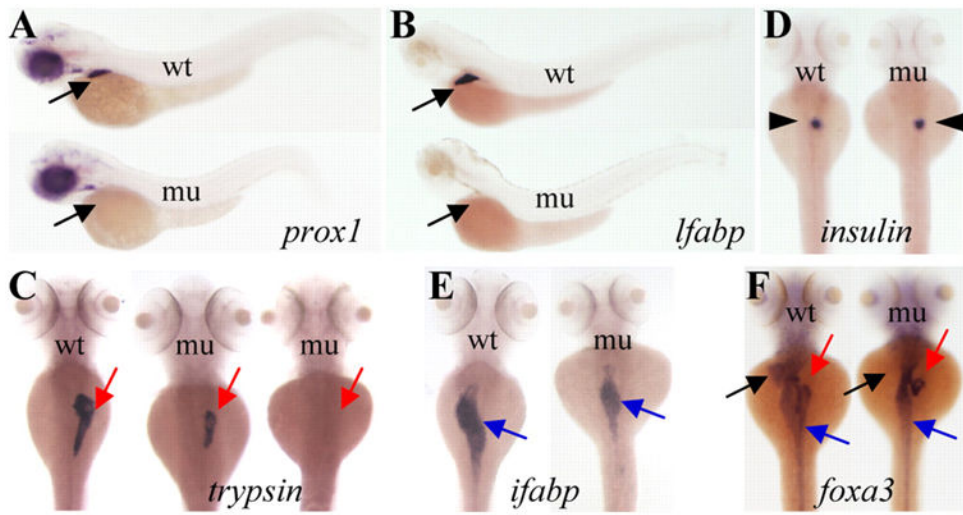
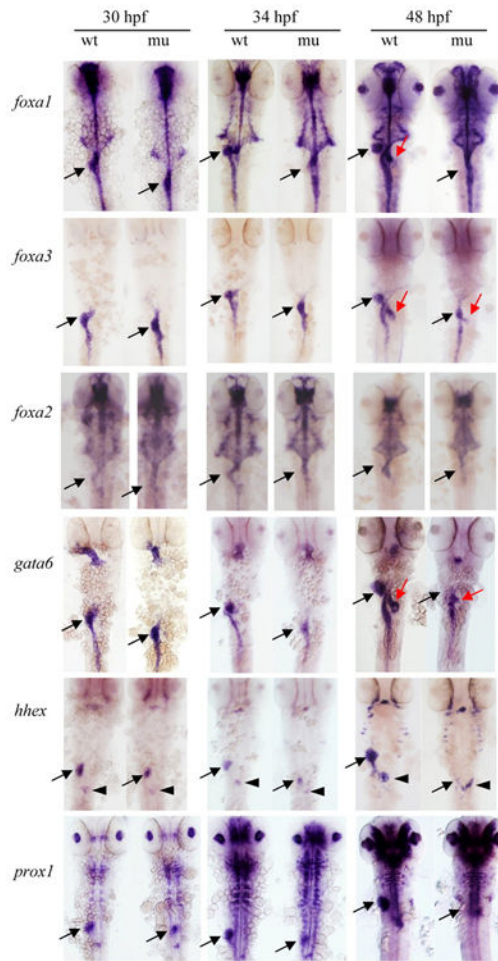
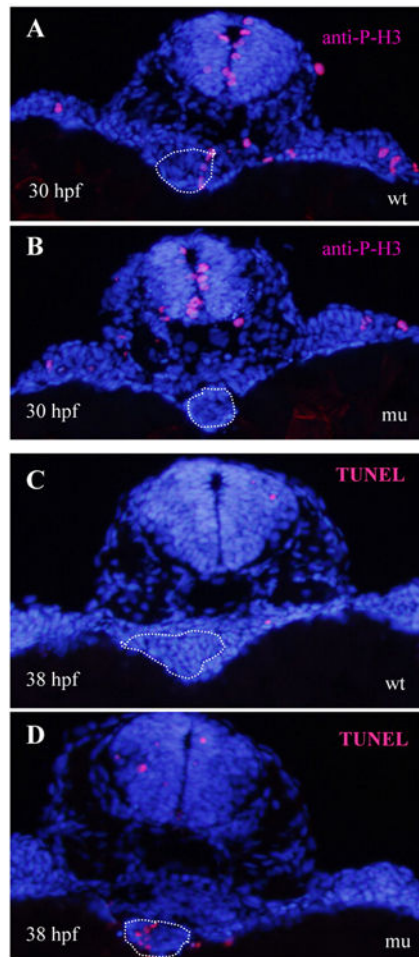


Figure 1.





**Figure 2.**



**Figure 3.**

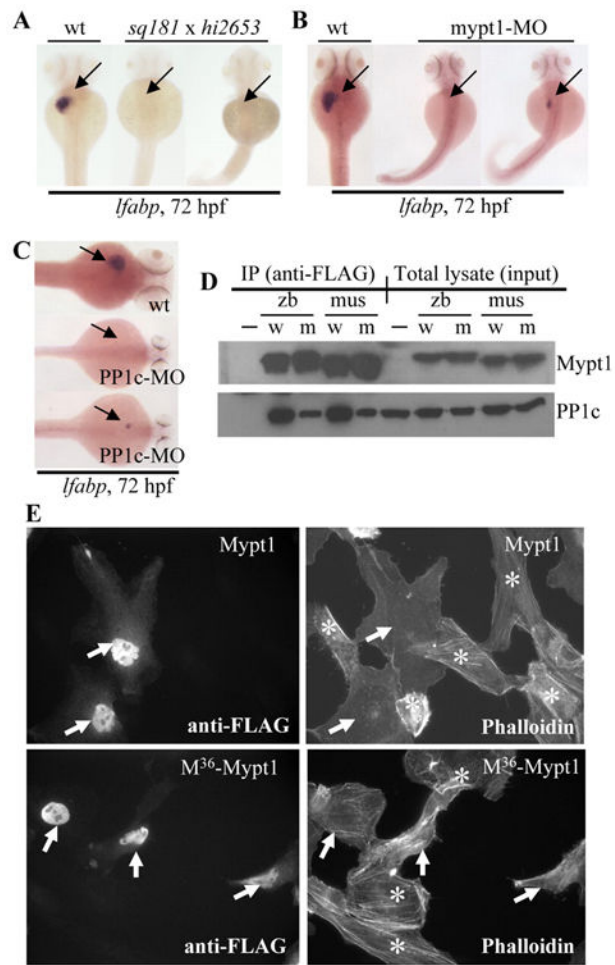


Figure 4.

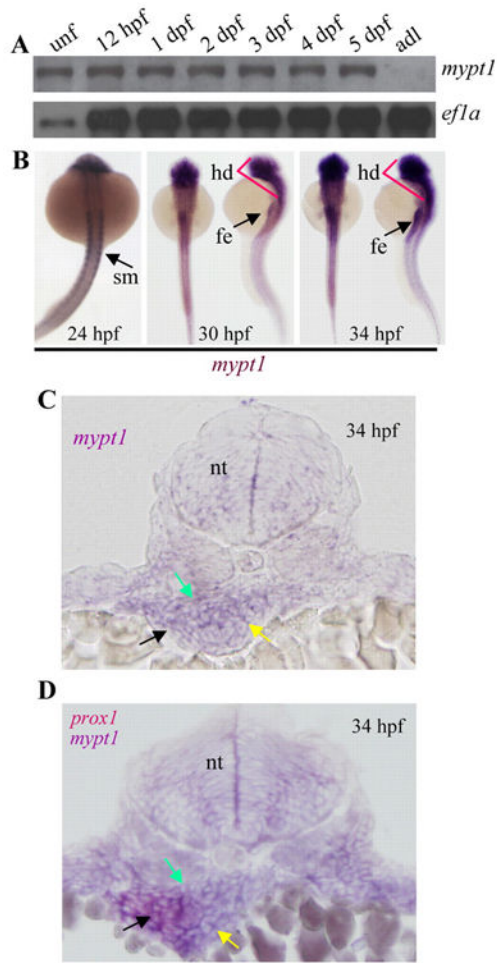


Figure 5.

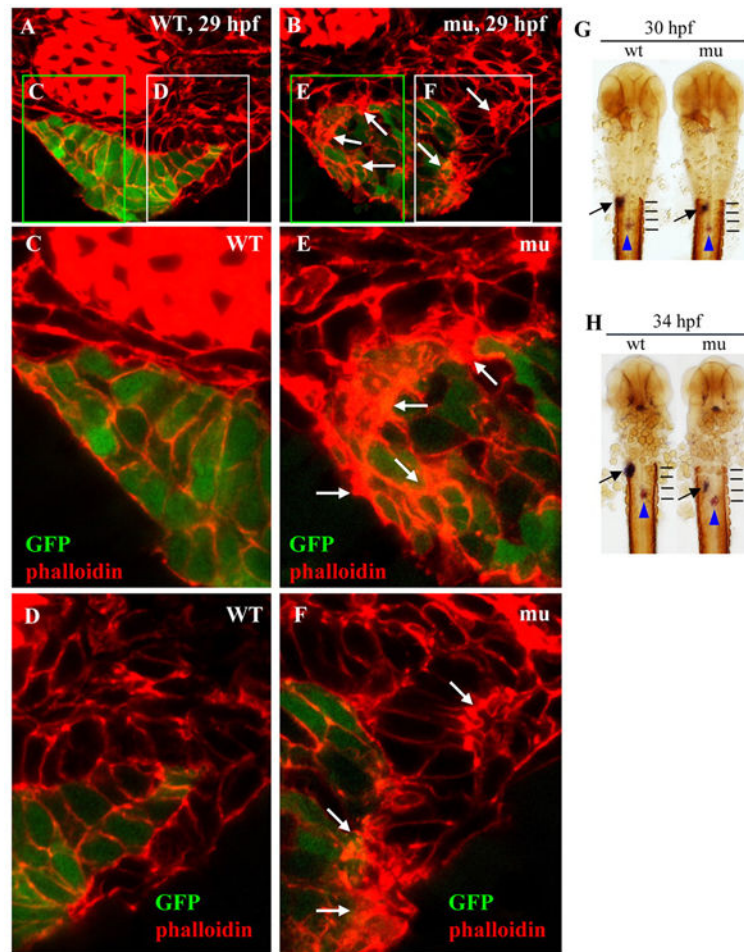


Figure 6.

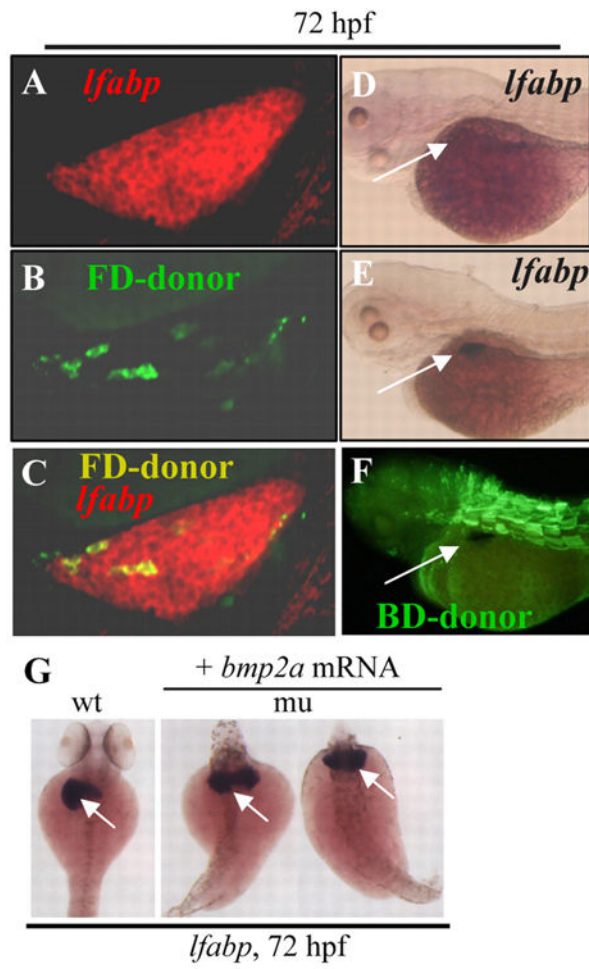


Figure 7.

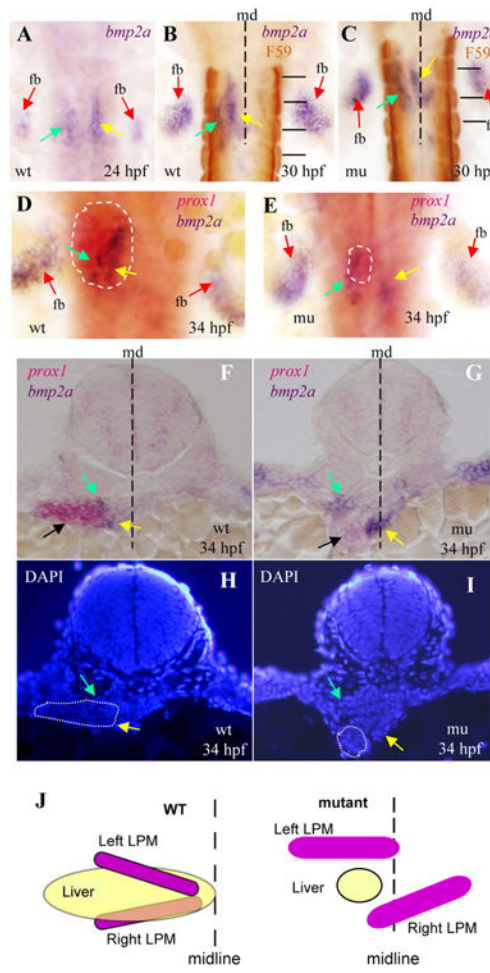


Figure 8.